THE JOURNAL OF BIOLOGICAL CHEMISTRY VOL. 285, NO. 40, pp. 30615–30621, October 1, 2010
© 2010 by The American Society for Biochemistry and Molecular Biology, Inc. Printed in the U.S.A.

X-ray Crystal Structure of the Bacterial Conjugation Factor PsiB, a Negative Regulator of RecA*

Received for publication, June 7, 2010 Published, JBC Papers in Press, July 21, 2010, DOI 10.1074/jbc.M110.152298

Vessela Petrova[‡], Kenneth A. Satyshur[§], Nicholas P. George[§], Darrell McCaslin[¶], Michael M. Cox[‡¶], and James L. Keck[§1]

From the [‡]Program in Cellular and Molecular Biology and Departments of [§]Biomolecular Chemistry and [¶]Biochemistry, University of Wisconsin, Madison, Wisconsin 53706-1532

During bacterial conjugation, genetic material from one cell is transferred to another as single-stranded DNA. The introduction of single-stranded DNA into the recipient cell would ordinarily trigger a potentially deleterious transcriptional response called SOS, which is initiated by RecA protein filaments formed on the DNA. During F plasmid conjugation, however, the SOS response is suppressed by PsiB, an F-plasmid-encoded protein that binds and sequesters free RecA to prevent filament formation. Among the many characterized RecA modulator proteins, PsiB is unique in using sequestration as an inhibitory mechanism. We describe the crystal structure of PsiB from the *Escherichia coli* F plasmid. The stucture of PsiB is surprisingly similar to CapZ, a eukaryotic actin filament capping protein. Structure-directed neutralization of electronegative surfaces on PsiB abrogates RecA inhibition whereas neutralization of an electropositive surface element enhances PsiB inhibition of RecA. Together, these studies provide a first molecular view of PsiB and highlight its use as a reagent in studies of RecA activity.

The discovery of conjugation, the transfer of genetically diverse DNA between bacteria, was a foundational achievement in molecular genetic studies. In their seminal work, Tatum and Lederberg (1) showed that genes could be transferred between two *Escherichia coli* cells. This experiment and others pointed to the existence of a "fertility factor," or "F factor," that facilitates genetic transfer (2). The F factor is a conjugative plasmid that can incorporate host genomic DNA and transfer this genetic information to other bacteria, providing the recipient with alternative copies of genes (3, 4). Notably, conjugation is also a factor in the rapid spread of antibiotic resistance genes among human bacterial pathogens (5). The mechanisms underlying conjugation are therefore critical for bacterial genetic diversity and can limit the effectiveness of antibacterial therapies.

During conjugation, the *E. coli* F plasmid undergoes rolling circle replication to transfer single-stranded DNA (ssDNA)[2] from a donor to a recipient cell (3, 6). Although this is an efficient transfer mechanism, introduction of ssDNA into the recipient cell also presents a potential problem since ssDNA is the primary trigger for the SOS transcriptional response in bacterial cells. The SOS response aids in survival under DNA-damaging conditions by stimulating expression of many DNA repair and cell cycle control genes (7, 8). Unabated SOS signaling can lead to mutagenesis (9); accordingly SOS induction is heavily regulated.

At the molecular level, SOS induction is mediated by formation of RecA protein filaments on ssDNA. RecA/ssDNA nucleoprotein filaments trigger SOS induction by acting as co-proteases in the auto-catalytic cleavage of the LexA transcriptional repressor protein, thus derepressing the LexA regulon (10, 11). In addition to this role, *E. coli* RecA is a central protein in DNA recombination and translesion DNA synthesis (12, 13). Functionally and structurally related recombinases are found in all domains of life (14).

The F plasmid effectively suppresses the SOS response in recipient cells during conjugation. The suppression is mediated by the plasmid-encoded "Plasmid SOS Interference protein B," PsiB, the gene for which is transferred and expressed at high levels very early in the conjugation process (15–18). Unlike other known RecA regulator proteins (19), PsiB acts by preventing RecA from binding to DNA by binding free RecA (20). Interestingly, *psiB* genes are present on many conjugative plasmids, indicating their broad utility in DNA transfer reactions (16–18, 21).

To better understand the mechanism of action of PsiB, we have determined the x-ray crystal structure of the PsiB protein from the *E. coli* F plasmid and used the structure to guide biochemical experiments that investigate RecA regulation by PsiB. Consistent with solution studies, PsiB forms a homodimer that is stabilized by a large interface between protomers in the crystal structure. The PsiB monomer comprises a fold that is unexpectedly similar to that of the eukaryotic actin-binding protein CapZ. Structure-directed neutralization of electronegative surfaces on PsiB abrogate its inhibition of RecA stimulation of LexA-cleavage and RecA DNA-dependent ATPase activities. Similar changes to an electropositive surface element enhance PsiB inhibition of RecA. Together, our structural and func-

* This work was supported, in whole or in part, by National Institutes of Health Grants GM32335 (to M. M. C.) and GM068061 (to J. L. K.).

The atomic coordinates and structure factors (code 3NCT) have been deposited in the Protein Data Bank, Research Collaboratory for Structural Bioinformatics, Rutgers University, New Brunswick, NJ (http://www.rcsb.org/).

[1] To whom correspondence should be addressed: Dept. of Biomolecular Chemistry, University of Wisconsin School of Medicine and Public Health, 550 Medical Science Center, 1300 University Ave., Madison, WI 53706-1532. Tel.: 608-263-1815; Fax: 608-262-5253; E-mail: jlkeck@wisc.edu.

[2] The abbreviations used are: ssDNA, single-stranded DNA; SSB, ssDNA-binding protein.

Downloaded from www.jbc.org at University of Wisconsin-Madison, on December 15, 2010

tional studies define molecular features of PsiB that are critical for inhibition of RecA function. Given the unique PsiB RecA inhibition mechanism, these studies also highlight PsiB as a useful reagent for the study of RecA-mediated processes.

EXPERIMENTAL PROCEDURES

Proteins—E. coli F plasmid PsiB protein and PsiB variants were purified as previously described (20). A selenomethionine derivative of the PsiB protein (SeMet PsiB) was overexpressed as previously described (22) and purified using a modified procedure in which a polyethylene amine precipitation was added, a single chromatographic step (hydroxyapatite) was used for purification, and 1 mM tris(2-carboxyethyl)phosphine was used as a reducing agent. *E. coli* SSB, RecA, and LexA were purified as described previously (20).

Protein Crystallization and Structure Determination—SeMet PsiB (7 g/liter protein in 20 mM Tris-Cl (80% cation, pH 7.7), 50 mM KCl, 10% glycerol) was crystallized by suspending 1 μl of protein mixed with 1-μl well solution (136 mM sodium acetate, pH 5.2, 1.4% PEG 4000, 20% glycerol) over 1 ml of well solution in a hanging-drop vapor-diffusion experiment. Crystals formed over several days at room temperature and were frozen in liquid nitrogen directly from the drop. Crystals diffracted to 2.2 Å resolution with $P4_32_12$ symmetry and unit cell dimensions of a = b = 93.8 Å, c = 164.8 Å, consistent with four PsiB proteins per asymmetric unit (23).

The structure of SeMet PsiB was determined by single wavelength anomalous dispersion phasing (Table 1). Data were indexed and scaled with HKL2000 (24). Selenium atom identification, phasing, and solvent flattening using PHENIX SOLVE (25). The structure was built manually using COOT (26) and improved by refinement with REFMAC5 (27) and manual rebuilding. Coordinate and structure factor files have been deposited at the Protein Data Bank (PDB ID 3NCT).

Analytical Ultracentrifugation—A sample of PsiB was dialyzed overnight against 20 mM Tris, pH 7.5, 150 mM KCl, 1 mM EDTA, and diluted with dialysis buffer to create three samples at 17, 29, and 41 μM used in sedimentation equilibrium studies. Centrifugation was performed using a Beckman XLA analytical ultracentrifuge, with measurements carried out at 20 °C. PsiB protein gradients were monitored by measuring $A_{280\ nm}$; superimposible gradients recorded at least 3 h apart confirmed equilibrium. Equilibrium data were collected at speeds of 6,600, 9,600, 12,000, 21,000, and 34,000 rpm followed by high-speed depletion to quantify any non-sedimenting baseline absorbance. These varied between −0.008 and 0.001, and have minimal impact on the analysis. The density of the buffer at 20 °C was calculated using density increment polynomials to be 1.0062 g/ml (28). The partial specific volume of the PsiB was calculated from its amino acid sequence as 0.730 ml/g. All data were processed and analyzed using Beckman provided software or programs written for Igo Pro (Wavemetrics, Inc, Lake Oswego, OR). Semi-log absorbance data as a function of squared radial distance were linear for all PsiB samples at all speeds, suggesting the presence of a single homogenous species. The data were merged and globally fitted using models containing one or two molecular species (29). Models involving multiple species did not improve the fits and/or returned unrealistic values for the fitting parameters.

Circular Dichroism Spectroscopy—Samples were prepared in 10 mM Tris-Cl, pH 7.5. Circular dichroic spectra were recorded at 37 °C in 0.1 cm path length cells with an averaging time was 5 s at 1 nm steps with a bandpass of 1 nm. To convert to molar ellipticity, the molar concentration was multiplied by 144 to give the concentration of residues. Spectra were adjusted to zero baseline by averaging data between 315 and 320 nm.

RecA ATPase Assays—M13mp18 ssDNA (3 μM, nucleotides) was incubated with 0.5 μM *E. coli* SSB (monomer), 0 or 10 μM PsiB (or 10 μM PsiB variant) (monomer) and 3 mM ATP in 1xRecA buffer (25 mM Tris acetate (80% cation, pH 7.58), 3 mM potassium glutamate, 10 mM magnesium acetate, 5% glycerol, 1 mM DTT) in the presence of an ATP regeneration system (30) for 10 min at 37 °C. ATP hydrolysis was initiated by adding 2 μM RecA and was measured spectrophotometrically as described previously (30).

LexA Cleavage Assays—M13mp18 ssDNA (3 μM, nucleotides) was incubated for 10 min at 37 °C with 0.5 μM *E. coli* SSB (monomer), 10 μM PsiB variant (monomer), and 3 mM ATP in 25 mM Tris acetate 80% cation (pH 7.62), 3 mM potassium glutamate, 3 mM magnesium acetate, 5% glycerol, 1 mM DTT) in the presence of an ATP regeneration system. RecA (2 μM) was added to the reaction and incubated for 10 min. LexA (10 μM) was then added to start each reaction, and samples were withdrawn at 0, 45, 60, and 90 min. The samples were denatured in 2× Laemmli buffer and analyzed by SDS-PAGE on a 17% polyacrylamide gel.

Fluorescence Polarization Protein Binding Assays—PsiB variants were labeled with fluorescein isothiocyanate (FITC) dye as previously described (20). The concentrations of labeled PsiB variants used as probes were: 87 nM WT PsiB, 7 nM PsiB1, 73 nM PsiB2, or 9 nM PsiB3. The concentrations were chosen so that the starting probe intensity was at least four times higher than background; in all cases the PsiB variant concentrations were significantly lower than the concentrations of RecA required for complex formation. Each variant was incubated with RecA protein diluted in 20 mM Tris-Cl, pH 7.63, 10% glycerol, 0.1 g/L BSA, 1 mM DTT for 10 min at room temperature. Data points are the mean of three independent experiments, and error bars represent one standard error of the mean.

RESULTS

Crystal Structure of PsiB from the E. coli F Plasmid—We have determined the crystal structure of the PsiB protein from the *E. coli* F plasmid to 2.2 Å resolution (Fig. 1 and Table 1). Single-wavelength anomalous dispersion phasing and solvent flattening produced high-quality experimental electron density maps of a selenomethionine-substituted version of PsiB that readily facilitated model building (Fig. 1*B*). The crystal form contained four monomers of PsiB per asymmetric unit. Electron density for all but three to six N-terminal residues and one C-terminal residue was modeled for each monomer. Non-crystallographic symmetry constraints were not used during structure refinement to allow independent refinement of each monomer structure. The structure was refined with good bond geometry and crystallographic statistics (Table 1).

Downloaded from www.jbc.org at University of Wisconsin-Madison, on December 15, 2010

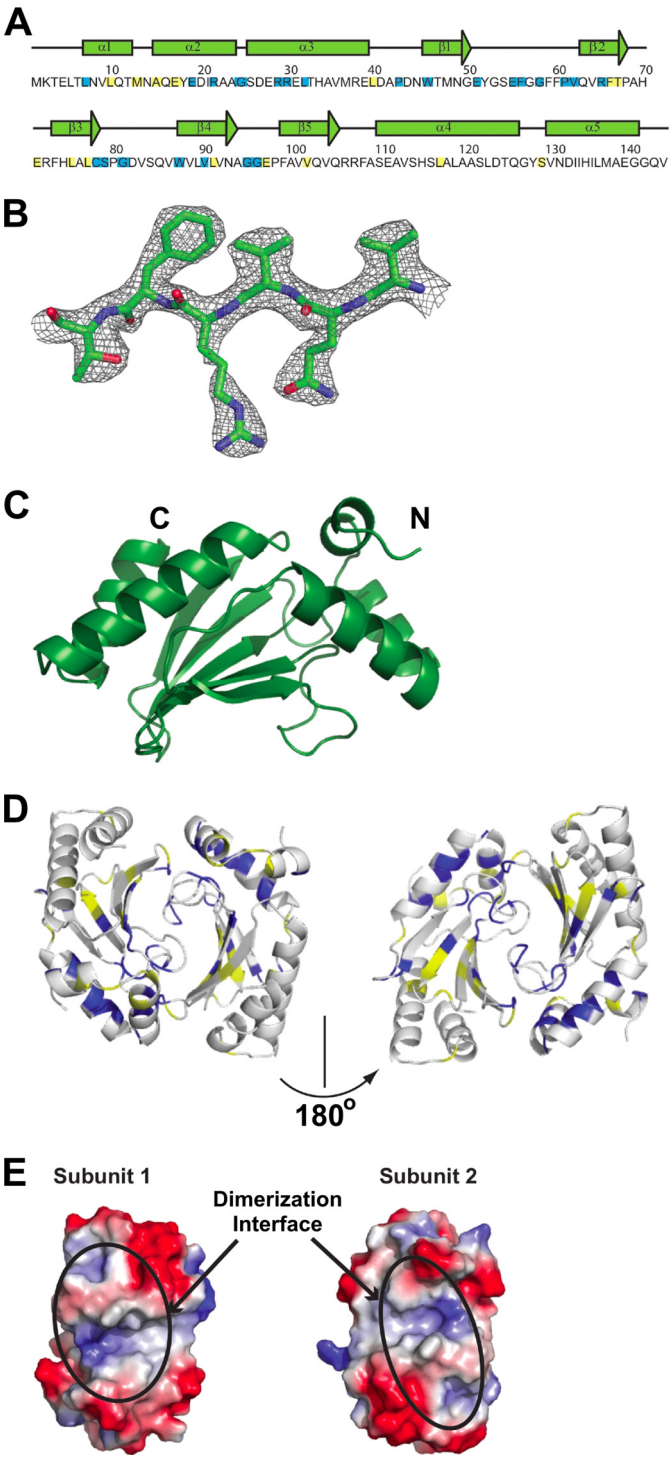


FIGURE 1. **Structure of the *E. coli* F plasmid PsiB protein.** *A*, PsiB primary and secondary structure. Conservation of sequences among conjugative plasmid PsiB proteins from *Escherichia coli*, *Shigella sonnei*, *Salmonella enterica*, *Pseudomonas entomophila*, and *Klebsiella pneumonia* is indicated with *blue* (invariant) or *yellow* (highly conserved) background on the PsiB sequence. Secondary structure is depicted as α-helices (*boxes*) and β-strands (*arrows*) above the PsiB sequence. *B*, view of a portion of the solvent-flattened experimental electron density map contoured to 2 σ superimposed with the refined PsiB structure. *C*, ribbon diagram of the crystal structure of the PsiB. *D*, ribbon diagram of the PsiB dimer. Conserved residues are colored as in *A*. *E*, electrostatic surface depiction of PsiB, highlighting the dimer interface. *Red* and *blue* depict electronegative and electropositive potential, respectively.

TABLE 1
Diffraction data and crystal structure solution

Data collection	
Wavelength, Å	0.97919
Resolution (last shell), Å	30-2.2 (2.24-2.20)
Number of reflections, measured/unique	428,553/71,325
Multiplicity	6.0 (5.9)
Completeness (last shell), %	99.8 (100)
R_{sym} [a] (last shell), %	5.9 (26.9)
I/σ (last shell)	22.0 (7.5)
Phasing statistics	
Resolution, Å	30-2.2
Figure of merit, before/after density modification	0.34/0.61
Refinement	
Resolution, Å	30-2.2
R_{work}/R_{free} [b], %	18.5/21.0
rms deviation bond lengths, Å	0.009
rms deviation bond angles, °	1.08
Ramachandran statistics (% most favored/ allowed/generously allowed/disallowed)	98.1/1.9/0/0

[a] $R_{sym} = \Sigma\Sigma j|Ij - <I>|\Sigma Ij$, where Ij is the intensity measurement for reflection j and $<I>$ is the mean intensity for multiply recorded reflections.
[b] $R_{work}/R_{free} = \Sigma||F_{obs}| - |F_{calc}||/|F_{obs}|$, where the working and free R factors are calculated by using the working and free reflection sets, respectively. The free R reflections (5% of the total) were held aside throughout refinement.

Each PsiB monomer in the crystal structure is comprised of a central five-stranded anti-parallel β sheet that is buttressed by α helices from the N and C termini (Fig. 1*C*). The β-strands and connecting loops curve to form a "C" shape in which the convex surface is packed against the helices. As is described further below, the concave surface forms a dimer interface with an adjacent PsiB protomer. Overlaying individual PsiB monomers from the crystallographic asymmetric unit shows that the structures are nearly identical; the root mean square deviation is 0.2 Å for 136 C_α atoms in the four molecules.

E. coli F Plasmid PsiB Protein Is a Dimer—Inspection of the protein packing revealed an arrangement in which pairs of PsiB proteins pack as dimers through a large, primarily hydrophobic interface (Fig. 1, *D* and *E*). The dimers further associate to form dimers of dimers through smaller interfaces. The major dimer interface buries 1975 $Å^2$ of surface area whereas the smaller interface buries only 825 $Å^2$ between proteins. The larger interface is evolutionarily well conserved among PsiB proteins whereas the smaller interface is not (Fig. 1*D*).

To determine whether PsiB was dimeric in solution, we used sedimentation equilibrium analytical centrifugation to measure the molecular mass of PsiB. Global fits of the data to a single molecular species converged on a weight average molecular mass of 31,227 ± 38 Da for PsiB. Because the PsiB monomer mass is 15,879 Da, these data are consistent with a dimeric quaternary structure for PsiB. No evidence for a monomer was observed, indicating that the K_d for dimerization is well below the lowest protein concentration tested (17 μM). Moreover, no evidence for higher order species (*e.g.* tetramer) was observed at the highest concentration tested (41 μM), suggesting that the tetrameric arrangement of PsiB in the crystallographic asymmetric unit is not representative of its oligomeric structure in solution. Together with the structural data presented above, these solution data support a dimeric structure for PsiB.

Structural Homology with CapZ, an Actin Filament Capping Protein—The PsiB protein fold was compared with other proteins in the Protein Data Bank using DALI to detect structurally homologous proteins (31). Despite the lack of significant

Downloaded from www.jbc.org at University of Wisconsin-Madison, on December 15, 2010

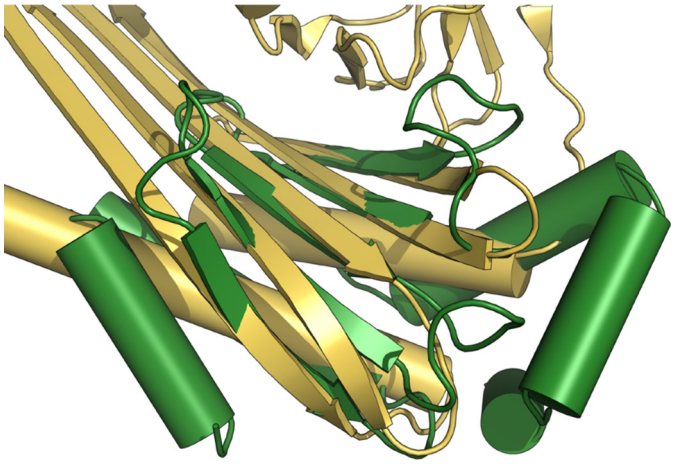


FIGURE 2. **Superposition of the structures of PsiB (*green*) with CapZ α (*gold*).**

sequence similarity, PsiB shares structural homology with a portion of the α and β subunits of the CapZ protein (32, 33) (Fig. 2). The root mean square deviation for common C_α atoms from PsiB and the CapZ α and β subunits is 3.4 Å and 3.9 Å, respectively, and both proteins share an α3-β5-α2 secondary structural arrangement that distinguishes PsiB and CapZ among proteins of known structure. Interestingly, the parallels between PsiB and CapZ extend beyond their folds. As is the case with PsiB, CapZ α/β heterodimers inhibit the function of a protein that acts as a filament (actin) (34) and the CapZ α/β interface is mediated by the β-sheet structure that is homologous with PsiB (32, 33). The actin interaction site of CapZ is localized to the C terminus of the β subunit of CapZ (35), which is not conserved with the structure of PsiB. It is unclear whether additional functional similarities exist between the two proteins.

Electrostatic PsiB Variants Identify Important Elements of the RecA-interaction Surface—The electrostatic surface of the PsiB dimer has two distinct areas of charge distribution. The first area has dense basic and acidic ridges whereas the opposite surface is more modestly charged (Fig. 3*A*, *left* and *right*, respectively). The importance of clustered charge elements for RecA auto-regulation (36) and for RecA regulation by other proteins (*e.g.* DinI, (37)) has been noted previously. The concentration of charges on one face of the PsiB dimer therefore led us to investigate whether these areas are important for PsiB interaction with and inhibition of RecA.

To probe the potential functional roles of PsiB electrostatic surfaces, three neutralizing PsiB variants were purified. The proteins neutralized combinations of acidic residues by substitution with alanines (PsiB1 (contains E17A, E19A, and D20A changes) and PsiB2 (contains E39A, D41A, and D44A changes)) or a combination of basic residues (PsiB3 (contains R106A and R107A changes)). The locations of the selected electrostatic regions on the surface of the PsiB dimer are shown in Fig. 3*A*. Circular dichroic spectra of the purified PsiB variants were indistinguishable from wild-type PsiB, confirming that the proteins were properly folded (Fig. 3*B*). Additionally, sedimentation equilibrium analytical centrifugation indicated that each variant was dimeric (data not shown), further confirming the integrity of the PsiB variants.

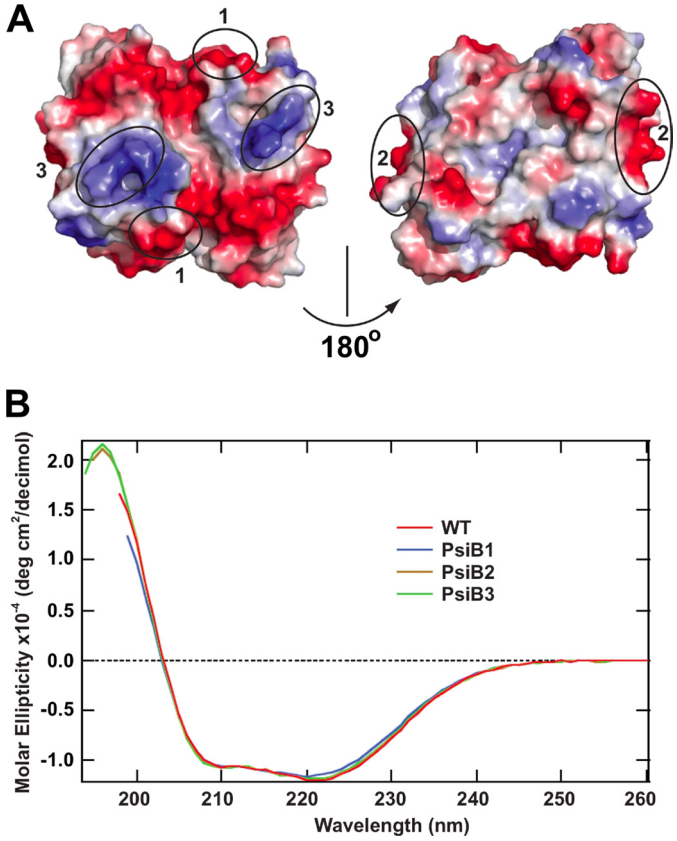


FIGURE 3. **Electrostatic surface of the PsiB dimer.** *A*, electrostatic views of the PsiB dimer. Electrostatic elements that are neutralized in PsiB variant proteins are indicated. *B*, circular dichroic spectra comparing wild-type PsiB and the three PsiB variants used in this study.

Neutralization of Electronegative Surfaces Diminishes PsiB Inhibition of RecA Function—Wild-type *E. coli* PsiB strongly inhibits RecA stimulation of LexA autocatalytic cleavage (20), which blocks induction of SOS *in vivo*. To test whether altering the electrostatic surfaces on PsiB affects this function, the PsiB variants were tested in an *in vitro* LexA cleavage assay (Fig. 4*A*). As observed previously, RecA-stimulated LexA proteolysis is efficient in the absence of PsiB but is strongly inhibited in the presence of wild-type PsiB. Strikingly, inhibition of RecA by PsiB1 and PsiB2 variants was greatly diminished relative to wild-type PsiB. These data indicate that acidic elements on the surface of PsiB are important for PsiB blockage of RecA-stimulated LexA cleavage. In contrast, neutralization of the basic PsiB surface in PsiB3 does not impair PsiB activity on RecA (Fig. 4*A*); indeed, PsiB3 appears to be slightly more potent as a RecA inhibitor because proteolytic product formation is reduced relative to the wild-type PsiB control.

To further explore the roles of PsiB electrostatic surfaces, the effects of the PsiB variants on RecA DNA-dependent ATPase activity were measured. The ATPase activity of *E. coli* RecA requires RecA filamentation on DNA, and provides an indirect measure of RecA protein binding to DNA (38). Consistent with earlier observations (20), the addition of wild-type PsiB strongly inhibits RecA ATPase activity (Fig. 4*B*). In contrast, both PsiB1 and PsiB2 had greatly diminished inhibitory effects on RecA ATPase activity. PsiB2 had almost no measurable inhibition activity whereas PsiB1 retained a very modest inhibitory effect.

Downloaded from www.jbc.org at University of Wisconsin-Madison, on December 15, 2010

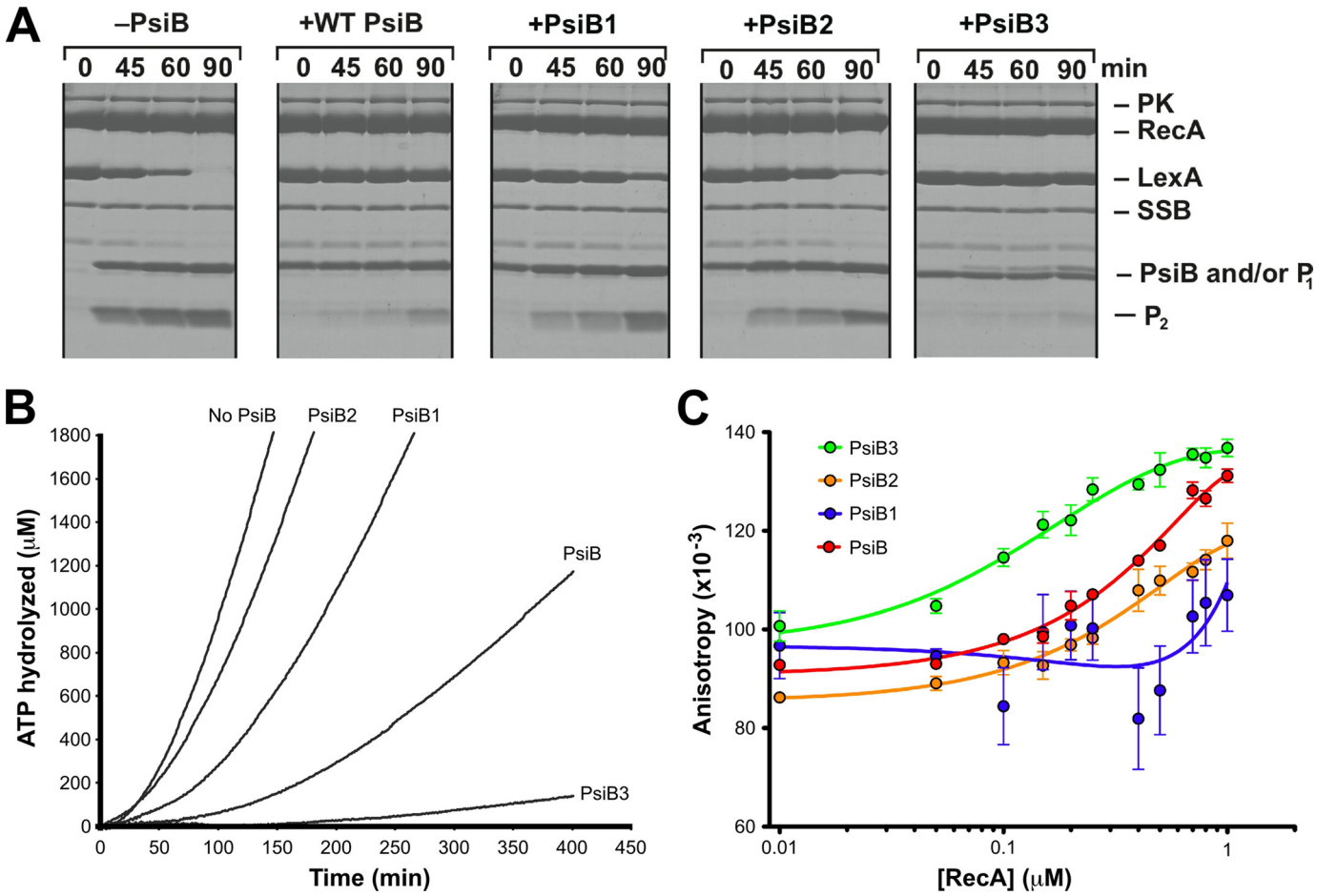


FIGURE 4. **Inhibition of RecA activites by PsiB variant proteins.** *A*, inhibition of RecA-stimulated LexA auto-proteolysis by PsiB variants. Gel mobility positions identify each of the components, including the ATP-regenerating system (*PK*) and LexA cleavage products, P_1 and P_2. *B*, inhibition of RecA DNA-dependent ATPase activity by PsiB variants. *C*, equilibrium binding isotherms of RecA association with FITC-labeled PsiB variants as monitored by fluorescence anisotropy. All data points are the average of three experiments. Error bars are one standard deviation from the mean.

However, PsiB3 exhibited an enhanced inhibition of the RecA ATPase activity relative to wild-type PsiB (Fig. 4*B*). Overall, the acidic surfaces of the PsiB appear to be critical for PsiB inhibition of RecA ATPase activity, whereas the basic surface appears to restrict the inhibitory activity of PsiB. These data parallel observations from the LexA cleavage assay.

Biochemically Impaired PsiB Proteins Appear to Form Less Stable Complexes with RecA—A simple hypothesis that could explain the RecA-dependent LexA cleavage and ATPase data is that the electronegative elements neutralized in the PsiB1 and PsiB2 variants are important for complex formation with RecA, whereas the electropositive surface neutralized in PsiB3 has a moderating role that weakens PsiB/RecA complex formation. To test this model directly, we initially attempted to label RecA with FITC for use in fluorescence polarization experiments with each of the PsiB variants. However, FITC-labeling of RecA rendered the protein inactive. We therefore labeled each of the PsiB variants with FITC and measured the change in fluorescence anisotropy of the labeled PsiB variant upon addition of RecA. Because this approach uses a different labeled protein in each titration, direct comparison of the binding behavior is limited to qualitative differences rather than a quantitative comparison stabilities. The FITC-labeled PsiB variants retained their inhibitory properties in DNA-dependent RecA ATPase activity assays (data not shown). Consistent with previous observations, RecA was able to bind FITC-PsiB (20). However, RecA appeared to bind the labeled FITC-PsiB1 and FITC-PsiB2 variants more weakly than it did FITC-PsiB, requiring higher RecA concentrations to reach the same fluorescence anisotropy levels in the variants than FITC-PsiB (Fig. 4*C*). In contrast, RecA appeared to bind to FITC-PsiB3 with higher affinity than to FITC-PsiB. These results qualitatively support a model in which neutralization of electronegative surfaces in PsiB1 or PsiB2 destabilize complex formation with RecA whereas neutralization of electronegative surfaces in PsiB3 produces a variant that forms a hyperstabilized complex with RecA. Moreover, these results are consistent with the differential effects of the PsiB variants in RecA inhibition studies.

DISCUSSION

The process of F plasmid conjugation in *E. coli* depends on PsiB to suppress RecA activities. A simple sequestration mechanism in which PsiB binds to free RecA to prevent RecA filament formation on DNA has been proposed (20) but the structural basis underlying PsiB activity has been unclear due to the lack of structural information for PsiB.

Downloaded from www.jbc.org at University of Wisconsin-Madison, on December 15, 2010

To better understand the mechanism of RecA inhibition by PsiB we have undertaken a structural and structure-based biochemical characterization of PsiB from the *E. coli* F plasmid.

The 2.2 Å-resolution crystal structure of PsiB revealed a C-shaped β-sheet core that is flanked on its convex surface by a helices (Fig. 1). The concave surface of the PsiB monomer is buried in a homodimeric interface with a second PsiB molecule. Solution studies confirmed a dimeric structure for PsiB. Comparison of the PsiB structure with other proteins revealed an unexpected structural similarity with CapZ, a eukaryotic actin capping protein (Fig. 2). Similarly to PsiB, CapZ functions as a dimer, although CapZ is an α/β heterodimer and uses a distinct surface from that of PsiB in dimer formation. The unexpected structural similarity between PsiB and CapZ may indicate that the two proteins are part of a broader family of proteins involved in the regulation of filamentous proteins.

The PsiB structure was used as a platform for creating three protein variants with altered electrostatic surfaces (Figs. 3 and 4). Relative to wild-type PsiB, PsiB variants with neutralized electronegative surfaces had reduced inhibitory activities in both RecA-catalyzed LexA autocleavage and DNA-dependent RecA ATPase activity assays and were defective in binding to RecA. These observations are consistent with the proposed sequestration mechanism of PsiB (20) and with the acidic elements forming important parts of the RecA binding site on PsiB.

Interestingly, neutralization of electropositive surfaces on PsiB makes the protein a more potent RecA inhibitor than wild-type PsiB, which appears to arise as a consequence of its increased affinity for RecA. These results implicate Arg-106 and Arg-107 of PsiB as playing a role in restraining RecA binding, which could help regulate PsiB activity. With its heightened potency, the PsiB3 protein is a useful tool for studying RecA activities by creating a soluble "RecA sink" that can bind free RecA in biochemical assays. All other characterized RecA inhibitors modulate the DNA-bound filamentous form of RecA rather than free RecA. Because filamentous RecA is its major active form, use of inhibitors that bind to the filaments can lead to unanticipated consequences in biochemical assays. However, with its strong effects on free RecA, PsiB3 may prove to be very useful in experimental studies of RecA filament dynamics or RecA applications in biotechnology.

RecA inhibition by PsiB has implications for the development of antibacterial therapeutics. The SOS response in bacteria contributes to the development of antibiotic resistance by inducing mutations through error-prone replication (39) and by promoting horizontal transfer of antibiotic resistance genes among bacteria (40). These properties have inspired searches for inhibitors that disrupt the SOS-inducing activities of RecA (41). The structural information presented herein describes key features of PsiB-mediated RecA inhibition that may be instructive for rational design of novel RecA inhibitors. Future studies that map the precise PsiB binding site on RecA will be required to aid these studies and to better understand PsiB's mechanism of action.

Acknowledgment—We thank Liz Wood for technical assistance.

REFERENCES

1. Tatum, E. L., and Lederberg, J. (1947) *J. Bact.* **53,** 673–684
2. Lederberg, J., and Tatum, E. L. (1953) *Science* **118,** 169–175
3. Willetts, N., and Skurray, R. (1987) in *Escherichia coli and Salmonella typhimurium: Cellular and Molecular Biology* (Neidhardt, F. C., Ingraham, J. L., Low, K. B., Magasanik, B., Schaeter, M., and Umbarger, H. E., eds), pp. 1110–1133, American Society for Microbiology, Washington DC
4. Frost, L. S., Ippen-Ihler, K., and Skurray, R. A. (1994) *Microbiol. Rev.* **58,** 162–210
5. de la Cruz, F., and Davies, J. (2000) *Trends Microbiol.* **8,** 128–133
6. Narra, H. P., and Ochman, H. (2006) *Curr. Biol.* **16,** R705–710
7. Sassanfar, M., and Roberts, J. W. (1990) *J. Mol. Biol.* **212,** 79–96
8. Courcelle, J., Khodursky, A., Peter, B., Brown, P. O., and Hanawalt, P. C. (2001) *Genetics* **158,** 41–64
9. Napolitano, R., Janel-Bintz, R., Wagner, J., and Fuchs, R. P. (2000) *EMBO J.* **19,** 6259–6265
10. Little, J. W., Edmiston, S. H., Pacelli, L. Z., and Mount, D. W. (1980) *Proc. Natl. Acad. Sci.* **77,** 3225–3229
11. Phizicky, E. M., and Roberts, J. W. (1981) *Cell* **25,** 259–267
12. Cox, M. M. (2007) in *Topics in Current Genetics: Molecular Genetics of Recombination* (Rothstein, R., and Aguilera, A., eds), pp. 53–94, Springer-Verlag, Heidelberg
13. Jiang, Q., Karata, K., Woodgate, R., Cox, M. M., and Goodman, M. F. (2009) *Nature* **460,** 359–363
14. Aravind, L., Walker, D. R., and Koonin, E. V. (1999) *Nucleic Acids Res.* **27,** 1223–1242
15. Bagdasarian, M., D'Ari, R., Filipowicz, W., and George, J. (1980) *J. Bacteriol.* **141,** 464–469
16. Bagdasarian, M., Bailone, A., Bagdasarian, M. M., Manning, P. A., Lurz, R., Timmis, K. N., and Devoret, R. (1986) *Proc. Natl. Acad. Sci. U. S. A.* **83,** 5723–5726
17. Bagdasarian, M., Bailone, A., Angulo, J. F., Scholz, P., and Devoret, R. (1992) *Mol. Microbiol.* **6,** 885–893
18. Althorpe, N. J., Chilley, P. M., Thomas, A. T., Brammar, W. J., and Wilkins, B. M. (1999) *Mol. Microbiol.* **31,** 133–142
19. Cox, M. M. (2007) *Crit. Rev. Biochem. Mol. Biol.* **42,** 41–63
20. Petrova, V., Chitteni-Pattu, S., Drees, J. C., Inman, R. B., and Cox, M. M. (2009) *Mol. Cell* **36,** 121–130
21. Golub, E., Bailone, A., and Devoret, R. (1988) *J. Bacteriol.* **170,** 4392–4394
22. Van Duyne, G. D., Standaert, R. F., Karplus, P. A., Schreiber, S. L., and Clardy, J. (1993) *J. Mol. Biol.* **229,** 105–124
23. Matthews, B. W. (1968) *J. Mol. Biol.* **33,** 491–497
24. Otwinowski, Z., and Minor, W. (1997) *Methods Enzymol.* **276,** 307–326
25. Terwilliger, T. (2004) *J. Synch. Rad.* **11,** 49–52
26. Emsley, P., and Cowtan, K. (2004) *Acta Crystallogr. D Biol. Crystallogr.* **60,** 2126–2132
27. Murshudov, G. N., Vagin, A. A., and Dodson, E. J. (1997) *Acta Crystallogr. D Biol. Crystallogr.* **53,** 240–255
28. Laue, T. M., and Shah, B. D. (1992) in *Analytical Ultracentrifugation in Biochemistry and Polymer Science* (Harding, S. E., Rowe, A. J., and Horton, J. C., eds) pp. 90–125, Royal Society of Chemistry, Cambridge
29. Laue, T. M. (1995) *Methods Enzymol.* **259,** 427–452
30. Lindsley, J. E., and Cox, M. M. (1989) *J. Mol. Biol.* **205,** 695–711
31. Holm, L., and Park, J. (2000) *Bioinformatics* **16,** 566–567
32. Yamashita, A., Maeda, K., and Maéda, Y. (2003) *EMBO J.* **22,** 1529–1538
33. Holm, L., Kääriäinen, S., Rosenström, P., and Schenkel, A. (2008) *Bioinformatics* **24,** 2780–2781
34. Caldwell, J. E., Heiss, S. G., Mermall, V., and Cooper, J. A. (1989) *Biochemistry* **28,** 8506–8514
35. Hug, C., Miller, T. M., Torres, M. A., Casella, J. F., and Cooper, J. A. (1992) *J. Cell Biol.* **116,** 923–931
36. Lusetti, S. L., Wood, E. A., Fleming, C. D., Modica, M. J., Korth, J., Abbott,

Downloaded from www.jbc.org at University of Wisconsin-Madison, on December 15, 2010

L., Dwyer, D. W., Roca, A. I., Inman, R. B., and Cox, M. M. (2003) *J. Biol. Chem.* **278,** 16372–16380
37. Voloshin, O. N., Ramirez, B. E., Bax, A., and Camerini-Otero, R. D. (2001) *Genes Dev.* **15,** 415–427
38. Cox, M. M. (2003) *Annu. Rev. Micro.* **57,** 551–577
39. Cirz, R. T., Chin, J. K., Andes, D. R., de Crécy-Lagard, V., Craig, W. A., and Romesberg, F. E. (2005) *PLoS Biol.* **3,** e176
40. Beaber, J. W., Hochhut, B., and Waldor, M. K. (2004) *Nature* **427,** 72–74
41. Wigle, T. J., Sexton, J. Z., Gromova, A. V., Hadimani, M. B., Hughes, M. A., Smith, G. R., Yeh, L. A., and Singleton, S. F. (2009) *J. Biomol. Screen* **14,** 1092–1101

Downloaded from www.jbc.org at University of Wisconsin-Madison, on December 15, 2010